Critical Behavior of Colloid-Polymer Mixtures in Random Porous Media

R. L. C. Vink,[1] K. Binder,[2] and H. Löwen[1]

[1]*Institut für Theoretische Physik II, Heinrich-Heine-Universität Düsseldorf, Universitätsstraße 1, 40225 Düsseldorf, Germany*
[2]*Institut für Physik, Johannes Gutenberg-Universität Mainz, Staudinger Weg 7, 55099 Mainz, Germany*

(Received 1 August 2006; published 6 December 2006)

We show that the critical behavior of a colloid-polymer mixture inside a random porous matrix of quenched hard spheres belongs to the universality class of the random-field Ising model. We also demonstrate that random-field effects in colloid-polymer mixtures are surprisingly strong. This makes these systems attractive candidates to study random-field behavior experimentally.

DOI: 10.1103/PhysRevLett.97.230603 PACS numbers: 05.70.Jk, 02.70.−c, 64.70.Fx, 82.70.Dd

One long-standing problem in the phase behavior of fluids concerns the universality class of the liquid-gas transition in random porous media. Conceivable universality classes are those of the pure Ising model, the (bond or site) diluted Ising model [1], or the random-field Ising model [2–4]. It was suggested by de Gennes [5] that the universality class is that of the random-field Ising model. However, resolving the universality class experimentally is difficult, partly because well-characterized porous media are scarce. The prototype realization is silica aerogel, which has the disadvantage that the coupling between the porous medium and the fluid is weak. This is evident from the small shift in the critical temperature observed in these systems [6,7]:

$$\delta \equiv |T_M - T_P|/T_P \approx 6 \times 10^{-3}, \qquad (1)$$

where T_P is the critical temperature in the pure system, and T_M the critical temperature in the aerogel matrix. The universality class, consequently, could not be resolved in these experiments.

In theoretical approaches, the porous medium is usually modeled by an equilibrium configuration of fixed spheres. The fluid particles are then allowed to migrate through the medium. Interestingly, these quenched-annealed systems display pronounced shifts in the critical temperature, typically $\delta > 0.2$ [8–13]. Compared to aerogel, the coupling between the fluid and the porous medium is thus much stronger, making quenched-annealed fluids attractive model systems.

Nevertheless, the universality class of quenched-annealed systems has not yet been determined. The most direct approach, which is to measure the critical exponents, is cumbersome because the critical exponents of the pure and diluted Ising model are rather similar, whereas for the random-field Ising model (RFIM), the critical exponents are not precisely known in any case. However, there is an additional feature in the critical behavior which can be used to resolve the universality class. A striking feature of the RFIM is that the standard hyperscaling relation between critical exponents is violated, and replaced by the modified relation $\gamma + 2\beta = \nu(d - \theta)$ [14,15]. Here, $d = 3$ is the spatial dimension; β, γ, and ν are the critical exponents of the order parameter, susceptibility, and correlation length, respectively, while θ is a third (probably not independent [16]) exponent called the ''violation of hyperscaling'' exponent. For the pure ($\beta \approx 0.326$; $\gamma \approx 1.239$; $\nu \approx 0.630$ [17]) and diluted ($\beta \approx 0.35$; $\gamma \approx 1.34$; $\nu \approx 0.68$ [1]) Ising models, hyperscaling is *not* violated, implying $\theta = 0$. In contrast, for the RFIM ($\beta < 0.13$; $\gamma \approx 1.7$–1.9; $\nu \approx 1.02$–1.1 [18,19]) one has $\theta \approx 1$.

The aim of this Letter is twofold. First, we demonstrate that hyperscaling is violated in quenched-annealed systems, using large-scale computer simulations and finite-size scaling. This fixes the critical behavior of quenched-annealed systems into the universality class of the RFIM, confirming the conjecture of de Gennes. Second, we show that quenched-annealed systems also pave the way toward exciting new experiments. As we will discuss, the considered quenched-annealed system is realized experimentally in a colloid-polymer mixture. Compared to aerogel, random-field effects should become easier to detect, due to the strong coupling between the fluid and the porous medium.

The outline of this Letter is as follows. First, we introduce our quenched-annealed model. Next, simulations are used to show that hyperscaling is violated. In addition, the critical exponents extracted from our data are shown to be compatible with those of the RFIM. Finally, we discuss how a quenched-annealed system can be realized experimentally in a colloid-polymer mixture.

We consider colloid-polymer mixtures within the framework of the Asakura-Oosawa-Vrij (AOV) model [20,21]. The AOV model is known to reproduce experimental observations remarkably well, including bulk phase separation [22], interfacial properties [23], and gelation [24]. In this model, colloids and polymers are treated as effective spheres of diameter σ_c and σ_p, respectively. The colloid-to-polymer size ratio is denoted as $q \equiv \sigma_p/\sigma_c$. Hard-sphere interactions are assumed between colloid-colloid and colloid-polymer pairs, while polymer-polymer pairs can interpenetrate freely. The simulations are performed in the grand canonical ensemble, where the volume V and the

respective (dimensionless) fugacities, z_c and z_p, of colloids and polymers are fixed, while the number of particles inside V fluctuates (lengths are expressed in units of σ_c). Following convention, the polymer fugacity is expressed by the polymer reservoir packing fraction $\eta_p^r = \pi z_p q^3/6$. The colloid packing fraction is $\eta_c = \pi\sigma_c^3 N_c/(6V)$, with N_c the number of colloids in the system. In the absence of quenched disorder, the phase behavior of the AOV model is well understood. For sufficiently large q, the AOV model phase separates into a colloid-rich phase (the colloidal liquid) and colloid-poor phase (the colloidal vapor), if η_p^r exceeds a critical value $\eta_{p,\mathrm{cr}}^r$ [25]. The binodal exhibits an Ising critical point [26]. The phase transition is driven by η_p^r, which thus plays a role similar to that of inverse temperature in liquid-vapor transitions of simple fluids.

We now consider the AOV model inside a random porous medium. The medium is modeled as an equilibrium ideal-gas configuration of spheres of diameter $\sigma_M = \sigma_c$ at fixed packing fraction $\eta_M = 0.05$ (in the terminology of Ref. [27], this resembles anticorrelated disorder). We set $q = 1.0$, assuming hard-sphere interactions between colloid-matrix pairs, while the polymer-matrix interaction is left ideal. We use a cubic simulation box of edge L with periodic boundary conditions. We aim to measure the order parameter distribution $[P_L]_{\mathrm{av}}$. Here, $P_L \equiv P_L(\eta_c)$ is the probability of observing a system with colloid packing fraction η_c measured for one realization of the matrix, while $[\cdots]_{\mathrm{av}}$ denotes an average over different matrix realizations. For each random matrix, a grand canonical Monte Carlo simulation of the AOV model is performed, using a cluster move [26]. Colloids and polymers are inserted and removed from the simulation box at random, with the constraint that colloid-colloid, colloid-polymer, and colloid-matrix overlaps are forbidden. During the simulations, the (quenched) matrix particles remain fixed. The number of colloids in the simulation box fluctuates, and this is used to measure $[\Delta F(N_c, N_c + 1)]_{\mathrm{av}}$, defined as the free energy difference between the state with N_c and $N_c + 1$ colloids, averaged over typically 250 matrix realizations. By successively measuring the free energy difference, the total averaged free energy $[W]_{\mathrm{av}}$ as a function of η_c results [28]. The latter is related to the sought-for distribution $[P_L]_{\mathrm{av}} \propto e^{-[W]_{\mathrm{av}}/k_B T}$, with k_B the Boltzmann constant and T the temperature.

At two-phase coexistence, $[P_L]_{\mathrm{av}}$ becomes double peaked, where the peak at low (high) η_c reflects the colloidal vapor (liquid) phase. The coexisting phase densities follow from the average peak positions. Typical distributions $[P_L]_{\mathrm{av}}$ are shown in the upper frame of Fig. 1, for several values of η_p^r. By recording the peak positions as a function of η_p^r, the binodal is found (see bottom frame). Unusual behavior is revealed. For pure Ising critical behavior, well-separated peaks in the order parameter distribution indicate that one is well away from the critical point, and inside the two-phase region of the

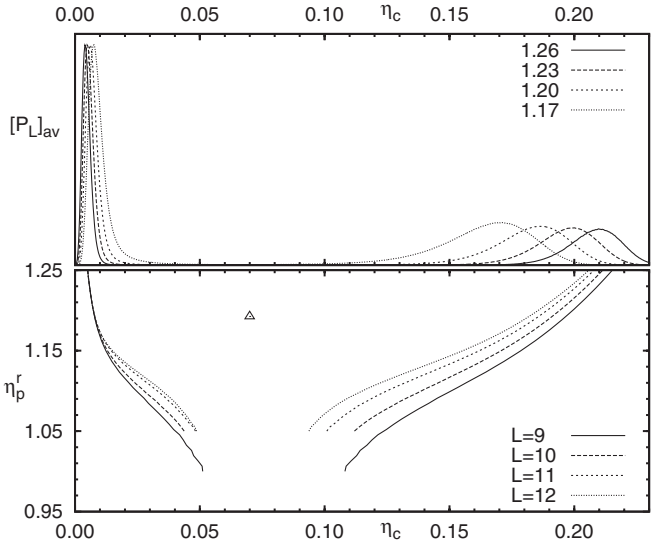

FIG. 1. Top frame: Order parameter distribution $[P_L]_{\mathrm{av}}$ for $L = 12$ and several values of η_p^r. Bottom frame: Binodal curves, obtained by reading off the peak positions in $[P_L]_{\mathrm{av}}$, for several system sizes L. The triangle at $\eta_{c,\mathrm{cr}} \approx 0.070$ and $\eta_{p,\mathrm{cr}}^r \approx 1.192$ marks the location of the critical point in the thermodynamic limit.

phase diagram. Finite-size effects in the peak positions should then be small. In contrast, even though the peaks in $[P_L]_{\mathrm{av}}$ are well separated for $\eta_p^r \approx 1.17$ and higher, the binodal continues to display a pronounced L dependence. To locate the critical point, we have measured the L dependence of the cumulant $U_1 \equiv [\langle m^2\rangle]_{\mathrm{av}}/[\langle|m|\rangle]_{\mathrm{av}}^2$ with $m = |\eta_c - [\langle\eta_c\rangle]_{\mathrm{av}}|$. At the critical point, the cumulant becomes system-size independent [29]. Plots of U_1 vs η_p^r, for several system sizes L, are expected to show a common intersection point, leading to an estimate of $\eta_{p,\mathrm{cr}}^r$. The result is shown in the top frame of Fig. 2, yielding $\eta_{p,\mathrm{cr}}^r = 1.192 \pm 0.005$. To determine the critical colloid packing fraction $\eta_{c,\mathrm{cr}}$, the quantity $[\langle\eta_c\rangle]_{\mathrm{av}}(L)$ evaluated at $\eta_{p,\mathrm{cr}}^r$, was linearly extrapolated in $1/L$, yielding $\eta_{c,\mathrm{cr}} \approx 0.070$.

We thus find that the order parameter distribution at the critical point remains sharp, featuring two well-separated and nonoverlapping peaks. Violation of hyperscaling then follows from the L dependence of the peak positions and the root-mean-square peak widths [30,31]. For the difference Δ between the liquid and vapor peak positions, finite-size scaling predicts $\Delta \propto L^{-\beta/\nu}$. Similarly, for the width χ of the vapor or liquid peak $\chi \propto L^{(\gamma/\nu - d)/2}$. The relative peak width thus becomes $w_r \equiv \chi/\Delta \propto L^{\omega}$ with $\omega = (\gamma/\nu - d)/2 + \beta/\nu$. In case hyperscaling holds $\omega = 0$, and a finite relative width $w_r > 0$ in the thermodynamic limit $L \to \infty$ is retained. In contrast, when hyperscaling is violated and $\omega < 0$, w_r vanishes in the thermodynamic limit, leading to an order parameter distribution featuring two δ peaks. Substitution of the RFIM critical exponents indeed yields $\omega < 0$, implying $w_r \to 0$ for $L \to \infty$, con-

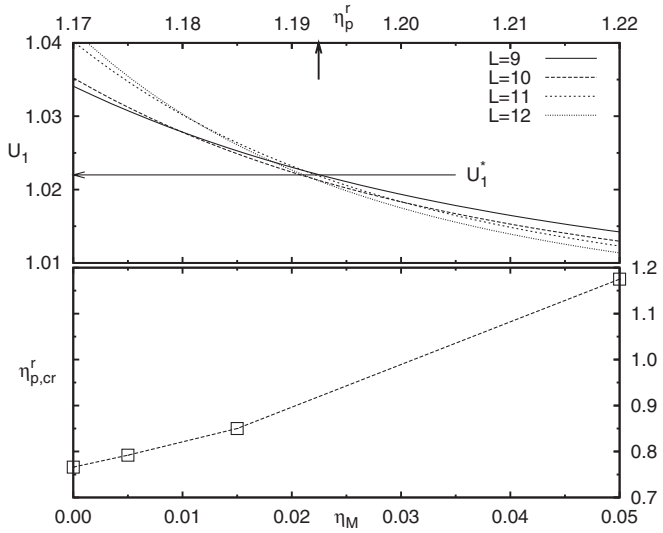

FIG. 2. Top frame: Cumulant analysis of the AOV model inside a porous medium at $\eta_M = 0.05$. Shown is U_1 vs η_p^r for several system sizes L. The vertical arrow marks our best estimate of $\eta_{p,\mathrm{cr}}^r$; the horizontal arrow defines $U_1^\star$. Bottom frame: $\eta_{p,\mathrm{cr}}^r$ as a function of η_M; the line serves to guide the eye.

sistent with our observations. Moreover, since the critical order parameter distribution tends to a sum of two δ peaks, the value $U_1^\star$ of the cumulant *at* the critical point (horizontal arrow in Fig. 2) approaches the trivial value $U_1 = 1$. Indeed, the cumulants of Fig. 2 intersect at a value close to 1, consistent with RFIM critical behavior, but ruling out pure and diluted Ising critical behavior, where $U_1^\star$ is significantly different from unity (see also Fig. 3).

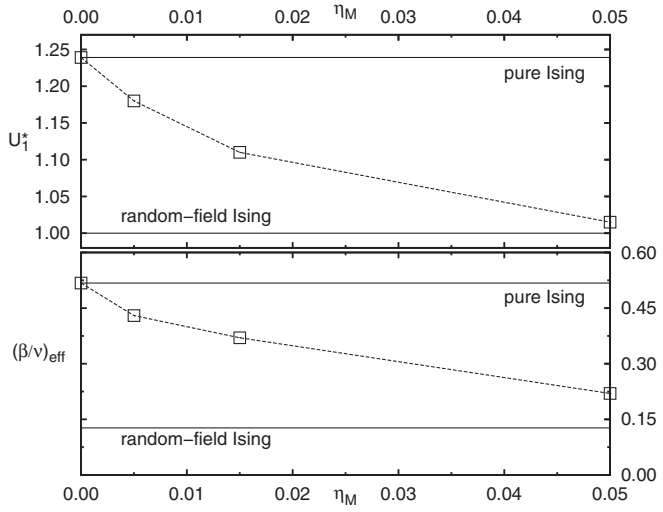

FIG. 3. Evidence of the crossover in critical behavior, from pure Ising toward random-field Ising, as a function of η_M. The top frame shows $U_1^\star$ as a function of η_M. The bottom frame shows the effective critical exponent ratio β/ν as a function of η_M. The dashed lines serve to guide the eye; horizontal lines show pure Ising and RFIM values.

Having established that quenched-annealed systems show RFIM critical behavior, the experimental realization of such a model will be discussed. To this end, the crossover in critical behavior [32,33], from pure Ising to RFIM, must be addressed. Defining t as the relative distance from the critical point, the approach to the critical point, at $t = 0$, is characterized by two regimes: $t < t_x$ and $t > t_x$, with t_x the crossover temperature. For fluids in porous media, RFIM critical behavior is observed only when $t < t_x$. For $t > t_x$, the critical behavior is still dominated by the pure Ising model, and "effective" critical behavior is observed instead (in this case a combination of RFIM and pure Ising universality). Whether RFIM critical behavior can be observed depends crucially on t_x. If t_x is very small, precise temperature control is required, which may be difficult to realize experimentally. Note that t_x is a nonuniversal quantity, dependent on the particle interactions, and, most importantly, on the packing fraction of the porous medium η_M. By increasing η_M, random-field effects are expected to become more pronounced, implying a larger t_x. For silica aerogel, t_x is clearly very small, since the measured critical exponents do not differ much from those of the pure Ising model [6,7]. In contrast, our results for the quenched-annealed model show pronounced RFIM behavior, indicating a much larger t_x. For experimental applications, it then becomes relevant to know which values of η_M are required, in order to enable measurements in the regime $t < t_x$ and to observe RFIM behavior.

Shown in the bottom frame of Fig. 2 is $\eta_{p,\mathrm{cr}}^r$ as a function of η_M [34]. Defining the analogue of Eq. (1) as $\delta \equiv |\eta_{p,\mathrm{cr}}^r(M) - \eta_{p,\mathrm{cr}}^r(P)|/\eta_{p,\mathrm{cr}}^r(P)$, with $\eta_{p,\mathrm{cr}}^r(M)$ the critical value of η_p^r in the presence of the random matrix, and $\eta_{p,\mathrm{cr}}^r(P)$ the corresponding value in the pure ($\eta_M = 0$) system, δ is found to increase from $\delta \approx 0.03$ ($\eta_M = 0.005$) up to $\delta \approx 0.5$ ($\eta_M = 0.05$). This confirms our expectation that, by increasing η_M, random-field effects grow stronger, and t_x becomes larger. Evidence for the crossover in critical behavior is presented in the top frame of Fig. 3. Shown is $U_1^\star$ as a function of η_M. Recall that $U_1^\star$ is defined as the value of the cumulant at the critical point; see the top frame of Fig. 2. The horizontal lines correspond to $U_{1,\mathrm{pure}}^\star \approx 1.2391$ [35] of the pure Ising model, and the (exact) RFIM value $U_1^\star = 1$. The figure strikingly illustrates effective critical behavior, between that of the pure Ising model and the RFIM, with a pronounced drift toward the latter, as η_M increases. Additional confirmation of the crossover is obtained from the critical exponent ratio β/ν. Shown in the bottom frame of Fig. 3 is β/ν as a function of η_M. The upper horizontal line shows the pure Ising value; the lower line is an upper bound for the corresponding RFIM value [18,19]. Again, a clear drift toward the RFIM value is observed.

Figure 3 then provides a clear indication which value of η_M to use in an experiment. The relative distance from the critical point that can be reached in simulations is nowa-

days $t \approx 10^{-3}$ [36]; similar precision is also achieved in experimental colloid-polymer systems [37]. Although this precision is rather low compared to what is achieved in atomic fluids, Fig. 3 nevertheless shows pronounced deviations from pure Ising behavior already at $\eta_M = 0.015$, with the crossover to RFIM being nearly completed at $\eta_M = 0.05$. This suggests $\eta_M > 0.05$ as the optimal regime for experiments. Such packing fractions are surprisingly low and easily realized in aggregated colloidal rods [38] or spheres [39]. There may even be the exciting possibility to generate the porous medium by optically trapping some of the colloidal particles [40]. An additional advantage is that colloidal particles, due to their mesoscopic size, allow for very detailed investigations of fluid phase behavior. By using confocal microscopy, individual particles can be visualized and tracked directly in real space [41]. This has already enabled particle-level investigations of interface fluctuations [42] and bulk critical behavior [37]. The present results indicate that the experimental verification of random-field behavior is feasible in colloid-polymer mixtures.

In summary, we have used large-scale Monte Carlo simulations to resolve the universality class of the quenched-annealed model. The universality class was shown to be that of the random-field Ising model, as was evident from the violation of hyperscaling and the behavior of (effective) critical quantities. This confirms the conjecture of de Gennes. In addition, we have demonstrated the potential of colloid-polymer mixtures in the experimental detection of random-field critical behavior, providing a valuable alternative over aerogel-based systems.

This work was supported by the *Deutsche Forschungsgemeinschaft* under the SFB-TR6 (project sections D3 and A5). We thank M. Schmidt for stimulating discussions.

[1] P. E. Berche, C. Chatelain, B. Berche, and W. Janke, Eur. Phys. J. B **38**, 463 (2004).
[2] J. Z. Imbrie, Phys. Rev. Lett. **53**, 1747 (1984).
[3] Y. Imry and S.-k. Ma, Phys. Rev. Lett. **35**, 1399 (1975).
[4] T. Nattermann, in *Spin Glasses and Random Fields*, edited by A. P. Young (World Scientific, Singapore, 1998), p. 277.
[5] P. G. de Gennes, J. Phys. Chem. **88**, 6469 (1984).
[6] A. P. Y. Wong and M. H. W. Chan, Phys. Rev. Lett. **65**, 2567 (1990).
[7] A. P. Y. Wong, S. B. Kim, W. I. Goldburg, and M. H. W. Chan, Phys. Rev. Lett. **70**, 954 (1993).
[8] M. Álvarez, D. Levesque, and J.-J. Weis, Phys. Rev. E **60**, 5495 (1999).
[9] L. Sarkisov and P. A. Monson, Phys. Rev. E **61**, 7231 (2000).
[10] V. De Grandis, P. Gallo, and M. Rovere, Phys. Rev. E **70**, 061505 (2004).
[11] E. Schöll-Paschinger, D. Levesque, J.-J. Weis, and G. Kahl, Phys. Rev. E **64**, 011502 (2001).
[12] M. Schmidt, E. Schöll-Paschinger, J. Köfinger, and G. Kahl, J. Phys. Condens. Matter **14**, 12 099 (2002).
[13] E. Kierlik, M. L. Rosinberg, G. Tarjus, and P. A. Monson, J. Phys. Condens. Matter **8**, 9621 (1996).
[14] J. Villain, J. Phys. (Paris), Lett. **43**, L551 (1982).
[15] D. S. Fisher, Phys. Rev. Lett. **56**, 416 (1986).
[16] M. Gofman, J. Adler, A. Aharony, A. B. Harris, and M. Schwartz, Phys. Rev. Lett. **71**, 1569 (1993).
[17] M. E. Fisher and S.-Y. Zinn, J. Phys. A **31**, L629 (1998).
[18] H. Rieger, Phys. Rev. B **52**, 6659 (1995).
[19] M. E. J. Newman and G. T. Barkema, Phys. Rev. E **53**, 393 (1996).
[20] S. Asakura and F. Oosawa, J. Chem. Phys. **22**, 1255 (1954).
[21] A. Vrij, Pure Appl. Chem. **48**, 471 (1976).
[22] D. Aarts, R. Tuinier, and H. Lekkerkerker, J. Phys. Condens. Matter **14**, 7551 (2002).
[23] J. M. Brader, R. Evans, M. Schmidt, and H. Löwen, J. Phys. Condens. Matter **14**, L1 (2002).
[24] J. Bergenholtz, W. Poon, and M. Fuchs, Langmuir **19**, 4493 (2003).
[25] H. Lekkerkerker, W. Poon, P. Pusey, A. Stroobants, and P. Warren, Europhys. Lett. **20**, 559 (1992).
[26] R. L. C. Vink and J. Horbach, J. Chem. Phys. **121**, 3253 (2004).
[27] M. Schwartz, J. Villain, Y. Shapir, and T. Nattermann, Phys. Rev. B **48**, 3095 (1993).
[28] P. Virnau and M. Müller, J. Chem. Phys. **120**, 10 925 (2004).
[29] K. Binder, Z. Phys. B **43**, 119 (1981).
[30] K. Eichhorn and K. Binder, Europhys. Lett. **30**, 331 (1995).
[31] K. Eichhorn and K. Binder, J. Phys. Condens. Matter **8**, 5209 (1996).
[32] M. E. Fisher, Rev. Mod. Phys. **46**, 597 (1974).
[33] K. Binder and H.-P. Deutsch, Europhys. Lett. **18**, 667 (1992).
[34] For these data, we set $q = 0.8$, $\sigma_c = \sigma_M$, and also introduce hard-core matrix-polymer interactions.
[35] E. Luijten, M. E. Fisher, and A. Z. Panagiotopoulos, Phys. Rev. Lett. **88**, 185701 (2002).
[36] Y. C. Kim, M. E. Fisher, and E. Luijten, Phys. Rev. Lett. **91**, 065701 (2003).
[37] C. P. Royall, D. Aarts, and H. Tanaka, "Bridging Lengthscales in Colloidal Liquid-Vapour Interfaces: From Critical Divergence to Single Particles" (to be published).
[38] S. G. J. M. Kluijtmans, G. H. Koenderink, and A. P. Philipse, Phys. Rev. E **61**, 626 (2000).
[39] S. G. J. M. Kluijtmans and A. P. Philipse, Langmuir **15**, 1896 (1999).
[40] D. L. J. Vossen, A. van der Horst, M. Dogterom, and A. van Blaaderen, Rev. Sci. Instrum. **75**, 2960 (2004).
[41] A. van Blaaderen, Progr. Colloid Polym. Sci. **104**, 59 (1997).
[42] D. G. A. L. Aarts, M. Schmidt, and H. N. W. Lekkerkerker, Science **304**, 847 (2004).